

Anti-Jahn-Teller Polaron

Philip B. Allen and Vasil P. Perebeinos

Department of Physics and Astronomy, State University of New York, Stony Brook, New York 11794-3800
(May 19, 2019)

Distortions of the oxygen sublattice couple to e_g orbitals of Mn^{4+} and drive an E_g cooperative Jahn-Teller (orbital ordering) transition in $LaMnO_3$. Holes doped into this material form localized small polarons at a low threshold electron-phonon coupling, and give a consistent model for the insulating nature of lightly doped $LaMnO_3$, the anti-ferromagnetic to ferromagnetic transition, and then the metal-insulator transition as the doping is increased.

71.38.+i, 71.30.+h, 75.30.Vn

I. INTRODUCTION

The doped manganites $Re_{1-x}A_xMnO_3$ (where Re is typically La and A is typically Sr or Ca) have a fascinating (T, x) (temperature, concentration) phase diagram, including "colossal magnetoresistance" [1] when $T > 250K$ and $x > 0.20$. Experiment (transport [2], optical [3], diffraction [4], EXAFS [5], isotope studies [6]) and theory [7] indicate the appearance of polarons at this point in (T, x) . It is less well appreciated that small polarons are essential to explain the insulating phase at smaller x and $0K < T < 750K$ [8]. We offer a simple model for the cooperative Jahn-Teller (JT) transition in this part of the phase diagram. With no further adjustment of parameters, our model describes the polarons and the metal to insulator transition at $(T, x) \approx (0K, 0.15)$.

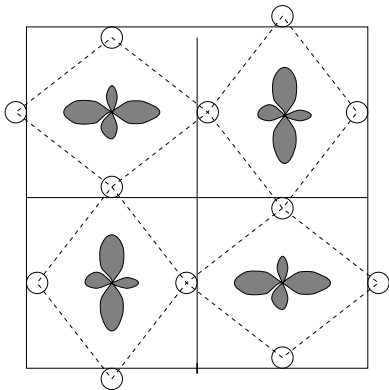


FIG. 1. Base plane (x - y plane) of Jahn-Teller distorted $LaMnO_3$. Rotations of oxygen octahedra are omitted, and distortions are exaggerated. Oxygens are displaced only along Mn-O-Mn bonds.

A canonical "Jahn-Teller polaron" [9] is the excess electron in $BaTiO_3$ [10], which sits in a triply degenerate

t_{2g} level. A local distortion of the lattice which splits the degenerate levels will then lower the energy and trap the electron in a small polaron state. By contrast, the polarons in $LaMnO_3$ are "anti-Jahn-Teller polarons." When pure, the valence is Mn^{3+} , with d^4 configuration in the high-spin state $t_{2g}^3 e_g^1$. A phase transition occurs at 750K [11] to a low-temperature structure with a cooperative JT distortion. Each e_g electron sits on a Mn atom surrounded by a local distortion of the oxygen octahedron illustrated schematically in Fig. 1. The distortions split the 2-fold e_g degeneracy; only the lower of the two orbitals on each site is occupied. When a hole is added, we show that a small polaron is formed by locally "undoing" [8] the JT distortion, pinning the hole onto a Mn^{4+} site with a filled t_{2g} shell.

As a model Hamiltonian we use $H = H_t + H_{ep} + H_L + H_U$.

$$H_t = t \sum_{\langle ij \rangle} c_x^\dagger(i) c_x(j) + H.C. + [x^\dagger y] + [y^\dagger z] \quad (1)$$

$$H_{ep} = \frac{4g}{3} \sum_{\langle ij \rangle} [c_x^\dagger(i) c_x(j) Q_x(j)] + [x^\dagger y] + [y^\dagger z] \quad (2)$$

$$H_L = \frac{K}{2} \sum_{\langle ij \rangle} [u_x(i)^2 + u_y(i)^2 + u_z(i)^2] \quad (3)$$

$$H_U = U \sum_i c_2^\dagger(i) c_2(i) c_3^\dagger(i) c_3(i) \quad (4)$$

The c^i operators create electrons whose spins (because of the large Hund's rule energy) are parallel to the $S = 3/2$ core spin, and hopping only operates between adjacent Mn sites with parallel spins. We use as a simplifying device an overcomplete basis for the two-dimensional e_g manifold, with orbitals $u_x = 3x^2 - r^2$, $u_y = 3y^2 - r^2$, and $u_z = 3z^2 - r^2$. Each of these orbitals points strongly along one of the Cartesian axes, and hops only along that direction. After re-expressing H_t in terms of the orthogonal orbitals $u_x / x^2 - y^2$ and $u_z / 3z^2 - r^2$, it turns out to be the correct nearest-neighbor two-center Slater-Koster [12] model, with $t = (dd\sigma)$, $(dd\pi)$ not entering due to symmetry, and $(dd\delta) = 0$. H.C. stands for Hermitian conjugate.

The variables $Q_x(\mathbf{k}) = u_x(\mathbf{k}) - u_x(\mathbf{k} - \hat{x})$ measure the local expansion of the oxygens on the x-axis around the n -th Mn atom. Such an expansion will lower the energy by $4g = \frac{1}{3}$ per unit Q_x and per unit occupancy of the orbital χ_x as shown in H_{ep} . The only lattice degree of freedom is oxygen motion along the direction of the bonds to the nearest two Mn atoms, with a harmonic restoring force $K u_x$. Kinetic energy is ignored, because we work in adiabatic approximation (oxygen mass = 1). Simultaneous occupancy by two orbitals is suppressed by a large ($U > 10t$) on-site repulsion. This model generalizes to e_g electrons the model of Rice and Sneddon [13] for s electrons in $BaBiO_3$. The same model, but with longer range forces, was used by Millis [14] for $LaMnO_3$.

First consider the unrealistic limit $U = 0$. Two magnetic states are of interest, antiferromagnetic (AFA, seen when $x < 0.1$), and ferromagnetic (Ferro, seen for $0.1 < x < 0.2$). In the Ferro state, electrons hop freely on a cubic lattice, while in the AFA state they are confined to the ferromagnetically polarized (001) planes, with hopping in the z-direction forbidden by the reversal of spin polarization. When $g = 0$ one diagonalizes H_t to find two bands with the symmetry property $\chi_1(\mathbf{k} + \mathbf{q}) = \chi_2(\mathbf{k})$, where $\mathbf{q} = (a)(1;1)$ or $(1,1,1)$ for AFA and Ferro. In both cases, the band is half-filled with $\nu_F = 0$, which guarantees perfect "nesting" at wavevector \mathbf{q} . Then an arbitrarily weak coupling g causes a cell-doubling JT transition, the weak-coupling version of the cooperative JT transition.

The electron-phonon term in the Hamiltonian (2) is conveniently split into Jahn-Teller and breathing parts, $H_{ep} = H_{JT} + H_{br}$:

$$H_{JT} = g \sum_{\mathbf{k}} \begin{pmatrix} c_2^y(\mathbf{k}); c_3^y(\mathbf{k}) \\ c_2^y(\mathbf{k}) & c_3^y(\mathbf{k}) \end{pmatrix} \begin{pmatrix} Q_3(\mathbf{k}) & Q_2(\mathbf{k}) \\ Q_2(\mathbf{k}) & Q_3(\mathbf{k}) \end{pmatrix} \begin{pmatrix} c_2(\mathbf{k}) \\ c_3(\mathbf{k}) \end{pmatrix} \quad (5)$$

$$H_{br} = \frac{P}{2} (1 + g) \sum_{\mathbf{k}} \begin{pmatrix} Q_1(\mathbf{k}) [c_2^y(\mathbf{k}) c_2(\mathbf{k}) + c_3^y(\mathbf{k}) c_3(\mathbf{k})] \end{pmatrix} \quad (6)$$

where the breathing amplitude is $Q_1 = \frac{P}{2} (Q_x + Q_y + Q_z)$, Q_2 is $Q_x - Q_y$, and Q_3 is $(2Q_z - Q_x - Q_y) = \frac{P}{3}$, in standard Van Vleck [15] notation. We allow a non-zero

following Millis, who recognized that additional charge coupling to the breathing mode was likely, beyond that contained in the starting Hamiltonian Eq.(2). However, to simplify the model, we set to zero in the following. Allowing a distortion $(Q_2; Q_3) = Q(\cos \theta; \sin \theta) \exp(i\mathbf{q} \cdot \mathbf{r})$, we re-diagonalize and minimize the sum of the elastic energy and the band energy. This yields optimal distortion parameters $Q; \theta$. The energy depends very weakly on θ unless we add anharmonic or strain terms to select more strongly a direction in $(Q_2; Q_3)$ -space. The upper panel of Fig. 2 shows the dependence of the dimensionless distortion $Q = gQ/t$ as a function of the dimensionless coupling $g = g/Kt$.

A more realistic case is the opposite limit $U = 1$. Here the electronic ground state has single occupancy of each site by a local orbital. If $g = 0$, each orbital is an arbitrary vector in $(\chi_2; \chi_3)$ -space. A non-zero g causes a cooperative ordering of the distortions Q and the orbitals. The optimal distortion has the same wavevector ($\mathbf{q} = (1; 1)$ or $(1; 1; 1)$) as in the $U = 0$ case, and $Q = 8g = K$ as shown below, but is independent of the angle θ in $(Q_2; Q_3)$ -space. Rather than introduce new parameters, we select the observed Q_2 -type distortion ($\theta = 0$) and proceed. It is convenient to make a 45 rotation in $(\chi_2; \chi_3)$ -space, to a new orthogonal basis,

$$\chi_x = \frac{1}{\sqrt{2}} (\chi_2 - \chi_3) = \frac{1}{\sqrt{2}} (\chi_x - \chi_y - \chi_z) \quad (7)$$

$$\chi_y = \frac{1}{\sqrt{2}} (\chi_2 + \chi_3) = \frac{1}{\sqrt{2}} (\chi_x + \chi_y - \chi_z) \quad (8)$$

where $(\chi_2; \chi_3) = (1/\sqrt{2})(1, 1, 1)$. The orbitals χ_x and χ_y point strongly in the \hat{x} and \hat{y} directions, and are equivalent under a 90 rotation in real space, as shown in Fig. 1. The part of H_{ep} which remains if $Q_3 = 0$ can be written as

$$H_{JT}^0 = g \sum_{\mathbf{k}} \begin{pmatrix} \chi_x(\mathbf{k}) \\ \chi_y(\mathbf{k}) \end{pmatrix} Q_2(\mathbf{k}) \begin{pmatrix} \chi_x(\mathbf{k}) \\ \chi_y(\mathbf{k}) \end{pmatrix} \quad (9)$$

where $\chi_x(\mathbf{k}) = c_x^y(\mathbf{k}) c_x(\mathbf{k}) - c_y^y(\mathbf{k}) c_y(\mathbf{k})$ measures the orbital order. At half filling the preferred distortion $Q_2(\mathbf{k}) = Q \exp(i\mathbf{q} \cdot \mathbf{r})$ alternates between $+Q$ (sublattice A) and $-Q$ (sublattice B). The corresponding electronic state has perfect orbital order:

$$|\mathcal{J}\rangle = \frac{1}{\sqrt{2}} \sum_{\mathbf{k}} \begin{pmatrix} \chi_x^A(\mathbf{k}) \\ \chi_x^B(\mathbf{k}) \end{pmatrix} c_x^y(\mathbf{k}) |\mathcal{J}\rangle \quad (10)$$

The energy is $\langle \mathcal{J} | H_{JT} | \mathcal{J} \rangle = N g Q + N K Q^2 = 16$ which comes from the JT and strain terms. The minimum value is $E = N = 4t$ which occurs at $Q = 8g = K$ as shown on Fig. 2. This JT phase is insulating, and should revert to an undistorted phase at a temperature $k_B T_c = t$. The gap to charge excitations (U) is large, but orbital excitations require only energy $16t$, and spin excitations occur down to low energies, with characteristic energy $J = t^2 = U$.

For intermediate values of U , exact solutions are no longer possible. If we use the wavefunctions Eq.(10) for large U and the band Slater determinant for small U as variational trial wavefunctions, then we find in the small U case a gradual enhancement of the JT distortion as U increases, and a crossover point, given in Fig. 2, where the two trial solutions have equal energy. Qualitatively the solutions found in the two regimes are not very different. The likely value of t is 0.3-0.4, t is of order 0.3eV, and U is of order 5eV. This puts $LaMnO_3$ on the strongly-correlated side of the boundary.

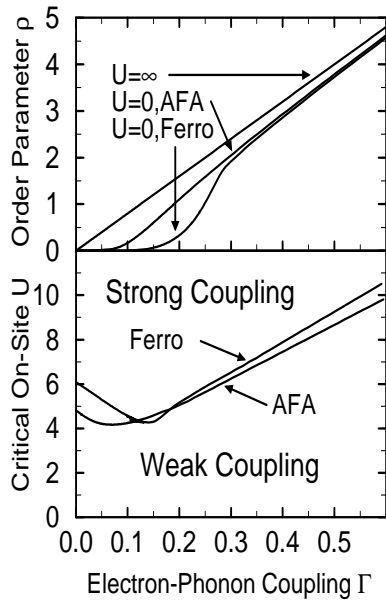


FIG. 2. Critical value of on-site repulsion U which separates weakly from strongly-correlated solutions. The upper panel shows the Jahn-Teller distortion $p = g^2/t$ as a function of $U = g^2/Kt$ for weak and strong-coupling solutions.

What happens when a hole is added? When $U = 0$ the hole is free to move, no matter how large is U , since spins are aligned in the planes. When $U > 0$ it costs energy $gQ = 8t$ in lost JT energy to remove the electron. There are two different ways to regain some energy. (a) At small g one expects an extended (metallic) solution with no relaxation of the Q_i 's. For $U = 1$ the wavefunction in first approximation is

$$|k\rangle = c_A \sum_{j^A} e^{ik \cdot r_{j^A}} |j^A\rangle + c_B \sum_{j^B} e^{ik \cdot r_{j^B}} |j^B\rangle \quad (11)$$

where the N states $|j^A\rangle$; $|j^B\rangle$ are obtained from $|j\rangle$ by putting the hole on a single site. The resulting kinetic energy is $\epsilon_k = t(1+2)(\cos k_x + \cos k_y)$ (AFA) with an additional term $\cos k_z$ in the Ferro case. The total energy of the hole then becomes $E_{h,ext} = t(8 - 1)$ (AFA) and $8 - 2$ (Ferro) at the optimum wavevector \mathbf{k} . (b) For large U there is more JT energy to be gained by readjusting Q_i than can be gained from delocalizing. The localized solution is non-metallic because a small impurity potential will pin it. The first approximation is to put the hole at a single site, for example an A site. The nearest \hat{x} -direction oxygens, instead of being displaced outwards by $u = 2g/K$, are now displaced inwards by $u = (4-3-1)g/K$, while the \hat{y} -oxygens, instead of being displaced inwards by $u = 2g/K$, are displaced slightly further inwards, by $u = (4-3+1)g/K$, and the \hat{z} -neighbors, formerly undisplaced, now are displaced in by $u = 4-3g/K$: The pattern of this anti-JT polaron is shown in Fig. 3. The net result is that the energy $E_{h,pol} = t$ needed to make the hole is reduced from 8 in

lost JT energy to 2 . This energy comes partly from a reduction in the strain cost and partly from energy of breathing. Setting $E_{h,ext} = E_{h,pol}$, we conclude that small polarons are stable for $U > 1=6$ in AFA phase, and that ferromagnetism, by enhancing the delocalization energy, prevents small polarons until $U > 1=3$. Experimentally, it is found that the Ferro phase for $0:10 < x < 0:15$ is insulating, but for $x > 0:15$ it becomes metallic. This is consistent with our model provided U is slightly larger than $1/3$. Increasing x eventually causes polaron overlaps and a metal to insulator transition at $x = 0:20$, presumably in a similar fashion to the description by Yu et al. [16] of doped $BaBiO_3$.

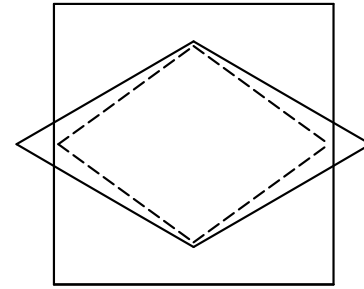


FIG. 3. Anti-Jahn-Teller polaron (dashed lines) in the x - y plane. The magnitude of the distortion is exaggerated, but the relative positions of O atoms (at vertices of rhombus) in the pure JT (solid line) state and in the polaron state are accurate.

The three largest errors in the calculation of the hole energy are (1) the localized hole can spread somewhat onto neighboring Mn atoms; (2) the Hilbert space for both localized and delocalized hole wavefunctions should include states with orbital defects (the hole is renormalized by coupling to "orbitons"); (3) the localized polaron in AFA phase will lower its energy further by causing spin canting on Mn atoms in adjacent planes, thus permitting interplanar hopping. Spin canting helps drive the AFA to Ferro transition at $x = 0:1$. We have calculated these effects by perturbation theory. The probability that a small hole polaron will be found away from the central site is $a/(1+a)$ where $a = 0:059 = t^2$ (AFA) and $0:099 = t^2$ (Ferro). At the smallest U where small polarons are stable, the probability is 17% and 9%. This shows that the small polaron is very well localized. The first two effects cause the energy to be lowered by Ct with small coefficients C similar in size for the localized and delocalized states. The shifts are small for values of $U > 0:2$. The critical value of U for small polaron formation changes from $U_c = 1=6$ to $0:170$ (AFA) and from $1/3$ to $0:319$ (Ferro). The third effect lowers the energy by $6 \times 10^{-5} t^2 = t^2 J$, causing a further small change in U_c .

To summarize, we examined a model with minimum parameters which allows a unified description of many of

the properties of LaMnO_3 and related compounds. Our work focussed on the cooperative Jahn-Teller state in the pure material, and the properties of a hole doped into this state. In the range of parameters appropriate for LaMnO_3 , this hole forms an anti-JT polaron, with surprisingly simple properties in the large U limit. Previous experience on the small U case BaBiO_3 [17] leads us to suspect that similar results should hold at small U , but the calculations are harder. We calculated the shift of the polaron energy due to orbital defects and spin canting; further details will be given in a longer paper. Numerous effects are left out of the model. Macroscopic strain, tilting of oxygen octahedra, and additional zero-point magnetic and non-adiabatic lattice fluctuations all could be added and would affect the $T = 0$ properties discussed here, but we believe that the effects we did include are the most important ones. A $T > 0$ treatment of all these effects is a bigger challenge. Perhaps more interesting would be an extension of the $T = 0$ calculations to higher doping where a remarkable variety of textured phases is being unravelled [18]. The properties of LaMnO_3 -related materials are incredibly rich, yet surprisingly understandable, in contrast to certain other transition-metal oxide systems.

ACKNOWLEDGMENTS

We thank W. Bao, M. B. Lum, D. E. Cox, J. P. Franck, J. B. Goodenough, J. P. Hill, D. I. Khomskii, and J.-S. Zhou for helpful conversations, and V. N. Kostur for the inspiration to start the project. This work was supported in part by NSF grant no. DMR-9725037.

-
- [1] G. Jonker and J. H. van Santen, *Physica (Amsterdam)* 16, 337 (1950); C. N. R. Rao and B. Raveau, editors, *Colossal Magnetoresistance, Charge Ordering, and Related Properties of Manganese Oxides*, World Scientific, Singapore, 1998.
- [2] M. Jain, M. B. Salamon, M. Rubinstein, R. E. Treece, J. S. Horowitz, and D. B. Chrisey, *Phys. Rev. B* 54, 11914 (1996); T. T. M. Palstra, A. P. Ramirez, S.-W. Cheong, B. R. Zegarski, P. Schier, and J. Zaanen, *Phys. Rev. B* 56, 5104 (1997); J. L. Cohn, J. J. Neumeier, C. P. Popoviciu, K. J. McClellan, and Th. Leventouri, *Phys. Rev. B* 56, R8495 (1997); J. P. Franck (private communication).
- [3] Y. Okimoto, T. Katsufuji, T. Ishikawa, A. Urushibara, T. Arima, and Y. Tokura, *Phys. Rev. Letters* 75, 109 (1995); K. H. Kim, J. H. Jung, and T. W. Noh, *Phys. Rev. Letters* 81, 1517 (1998); M. Quijada, J. Cerny, J. R. Simpson, H. D. Drew, K. H. Ahn, A. J. Millis, R. Shreekala, R. Ramesh, M. Rajeswari, and T. Venkatesan, *cond-mat/9803201*.
- [4] S. L. Billinge, R. G. D. Francesco, G. H. Kwei, J. J. Neumeier, and J. D. Thompson, *Phys. Rev. Letters* 77, 715 (1996); D. Louca, T. Egami, E. L. Brosha, H. Roder, and A. R. Bishop, *Phys. Rev. B* 56, 8475 (1997).
- [5] T. A. Tyson, J. Mustre de Leon, S. D. Conradson, A. R. Bishop, J. J. Neumeier, H. Roder, and J. Zang, *Phys. Rev. B* 53, 13985 (1996); A. Lanzara, N. L. Saini, M. Brunelli, F. Natali, A. Bianconi, P. G. Radaelli, and S.-W. Cheong, *Phys. Rev. Letters* 81, 878 (1998).
- [6] G.-m. Zhao, K. Conder, H. Keller, and K. A. Müller, *Nature* 381, 676 (1996).
- [7] A. J. Millis, P. B. Littlewood, and B. I. Shraiman, *Phys. Rev. Letters* 74, 5144 (1995); A. J. Millis, B. I. Shraiman, and R. Mueller, *Phys. Rev. Letters* 77, 175 (1996); A. J. Millis, R. Mueller, and B. I. Shraiman, *Phys. Rev. B* 54, 5389 and 5405 (1996); H. Roder, J. Zang, and A. R. Bishop, *Phys. Rev. Letters* 76, 1356 (1996); J. D. Lee and B. I. Min, *Phys. Rev. B* 55, 12454 (1997).
- [8] Y. Yamada, O. Hino, S. Nohdo, R. Kanao, T. Inami, and S. Katano, *Phys. Rev. Letters* 77, 904 (1996).
- [9] K. H. Hock, H. Nicksch, and H. Thomas, *Helv. Phys. Acta* 56, 237 (1983).
- [10] S. Kohne, O. F. Schirmer, H. Hesse, T. W. Kool, and V. Vikhnin, *J. Superconductivity* (in press).
- [11] J. B. Goodenough, A. Wold, R. J. Amott, and N. Menyuk, *Phys. Rev.* 124, 373 (1961); J. Rodriguez-Carvajal, M. Hennen, F. Moussa, A. H. Moudou, L. Pinsard, and A. Revcolevschi, *Phys. Rev. B* 57, 3189 (1998); Y. Murakami, J. P. Hill, D. Gibbs, M. B. Lum, I. Koyama, M. Tanaka, H. Kawata, T. Arima, Y. Tokura, K. Hirota, and Y. Endoh, *Phys. Rev. Lett.* 81, 582 (1998).
- [12] J. C. Slater and G. F. Koster, *Phys. Rev.* 94, 1498 (1954).
- [13] T. M. Rice and L. Sneddon, *Phys. Rev. Letters* 47, 689 (1982).
- [14] A. J. Millis, *Phys. Rev. B* 53, 8434 (1996).
- [15] J. H. Van Vleck, *J. Chem. Phys.* 7, 72 (1939); J. Kanamori, *J. Appl. Phys.* 31, 14S (1960); J. B. Goodenough, *Magnetism and the Chemical Bond*, Wiley Interscience, New York, 1963; p. 202; K. I. Kugel and D. I. Khomskii, *Sov. Phys. JETP* 37, 725 (1973).
- [16] J. Yu, X.-Y. Chen, and W. P. Su, *Phys. Rev. B* 41, 344 (1990).
- [17] P. B. Allen and V. N. Kostur, *Z. Phys. B* 104, 605-612 (1997).
- [18] W. Bao, J. D. Axe, C. H. Chen, and S.-W. Cheong, *Phys. Rev. Letters* 78, 543 (1997); P. G. Radaelli, D. E. Cox, M. Morez, and S.-W. Cheong, *Phys. Rev. B* 55, 3015 (1997); H. Kuwahara, Y. Morimoto, Y. Tomioka, A. Asamitsu, M. Kasai, R. Kumai, and Y. Tokura, *Phys. Rev. B* 56, 9386 (1997); S. Mori, C. H. Chen, and S.-W. Cheong, *Nature* 392, 473 (1998).